Methods of Oil Detection
in Response to the Deepwater Horizon Oil Spill

By Helen K. White, Robyn N. Conmy, Ian R. MacDonald, and Christopher M. Reddy

An in situ digital holographic camera (holocam) mounted on the front of a remotely operated vehicle deployed in the Gulf of Mexico in 2010 in response to the Deepwater Horizon oil spill. *Photo by Cabell S. Davis, © WHOI*

> "The northeastern Gulf of Mexico, where the surface oil was observed, encompasses 420,000 km^2 of coastal ocean, and it is likely that no previous oceanic event has had such sustained and intensive satellite observation over a similar area."

ABSTRACT. Detecting oil in the northern Gulf of Mexico following the Deepwater Horizon oil spill presented unique challenges due to the spatial and temporal extent of the spill and the subsequent dilution of oil in the environment. Over time, physical, chemical, and biological processes altered the composition of the oil, further complicating its detection. Reservoir fluid, containing gas and oil, released from the Macondo well was detected in surface and subsurface environments. Oil monitoring during and after the spill required a variety of technologies, including nimble adaptation of techniques developed for non-oil-related applications. The oil detection technologies employed varied in sensitivity, selectivity, strategy, cost, usability, expertise of user, and reliability. Innovative technologies ranging from remote sensing to laboratory analytical techniques were employed and produced new information relevant to oil spill detection, including the chemical characterization, the dispersion effectiveness, and the detection limits of oil. The challenge remains to transfer these new technologies to oil spill responders so that detection of oil following a spill can be improved.

INTRODUCTION

Oil detection during and after a spill is essential for spill response decision-making, environmental impact assessment, and understanding the ultimate fate of oil. During and after the Deepwater Horizon (DWH) oil spill in the Gulf of Mexico (GoM), multiple parties were engaged in detecting oil, including (1) federal and state agencies and the responsible party (in this case, BP) working in a coordinated response to mitigate the spill; (2) the Natural Resources Damage Assessment (NRDA) examining potential impacts of oil to ecosystems; and (3) the academic community who had a vested interest in both the response and the NRDA, and also in the science related to an 87-day release of reduced carbon into the GoM. The DWH spill produced an unparalleled amount of data (>50,000 oil analysis samples and thousands of data sets; NRDA public database, https://dwhdiver.orr.noaa.gov), and allowed for a variety of oil detection technologies to be employed, yielding significant advances in applied and basic science. Many discrete water and sediment samples are georeferenced, so that their collection locations are known to a high degree of accuracy. The resulting DWH database is 2.4 GB in size and contains over eight million georeferenced data points collected from industry, government databases, volunteer networks, and academic researchers (Thessen et al., 2016). The public availability of quality-assured data from industry and government is noteworthy, as this was not the practice for past spills. This has and will continue to allow analyses of these large data sets to understand the scope of the spill (e.g., Valentine et al., 2014; Boehm et al., 2016; Wade et al., 2016).

Measurements made by the academic community to detect oil in the GoM following the spill were initially funded by National Science Foundation Rapid Response Research (RAPID) grants; subsequently, the Gulf of Mexico Research Initiative provided funding that enabled scientists to examine data sets collected during the earliest stages of the spill and to evaluate the success of the technologies that were employed. Collaborations between government, industry, and academia continue to enhance the scientific and response community's understanding of oil transport, biogeochemical pathways, and fate.

The DWH spill released hot (105°C) reservoir fluid composed of 4.1 million barrels of liquid oil and 1.7×10^{11} g of C_1–C_5 hydrocarbon gases from the deep Macondo well over a period of 87 days (Reddy et al., 2012). Once in the water column, the reservoir fluid separated, forming subsurface plumes preferentially enriched with gases and the water-soluble components of the liquid oil (Joye et al., 2011; Reddy et al., 2012). Oil and gas trapped within deep subsurface waters was the immediate focus of scientists and responders (e.g., Joye et al., 2011, and references therein), although uncertainty remains regarding how much of the reservoir fluid remained in the subsurface (Ryerson et al., 2012). Established models predicted that 50%–95% of reservoir fluid could have been entrained in the subsurface, depending on the effect

of subsurface chemical dispersant application on oil droplet size distributions (Socolofsky et al., 2015). Hydrocarbon concentrations in the atmosphere, on the surface, and in the subsurface were used to estimate that 36% of the discharged reservoir fluid remained in the subsurface (Ryerson et al., 2012). These estimates may be refined with further research, but the presence of both subsurface and surface oil and gas compounds remains relevant. The fate of the hydrocarbon gases released in the DWH is quantitatively important, and methane was the most abundant compound released from the well (e.g., Reddy et al., 2012). This discussion will, however, focus on the detection of oil-derived hydrocarbons with six or more carbons (generically referred to as oil from here on). Detailed discussions regarding methods to detect these hydrocarbons, such as gas chromatography (GC) and high-resolution mass spectrometry are covered elsewhere (Tarr et al., 2016, in this issue).

A variety of oil detection technologies were employed during DWH to assess the spatial extent, quantify the release, and characterize the specific chemical and isotopic composition of the spilled oil. Oil that reached the surface ocean was detected by satellite, aircraft, buoy, glider, profiler, and surface vessel platforms (summarized in Figure 1 and highlighted in Figure 2). Subsurface detection of oil was conducted via in situ sensors deployed on profilers, gliders, remotely operated vehicles (ROVs), autonomous underwater vehicles (AUVs), and human-occupied deep submergence vehicles (e.g., DSV *Alvin*). Sensors included membrane inlet mass spectrometers (MS) to detect dissolved hydrocarbons, fluorometers to detect polycyclic aromatic hydrocarbons (dissolved and particulate combined) and
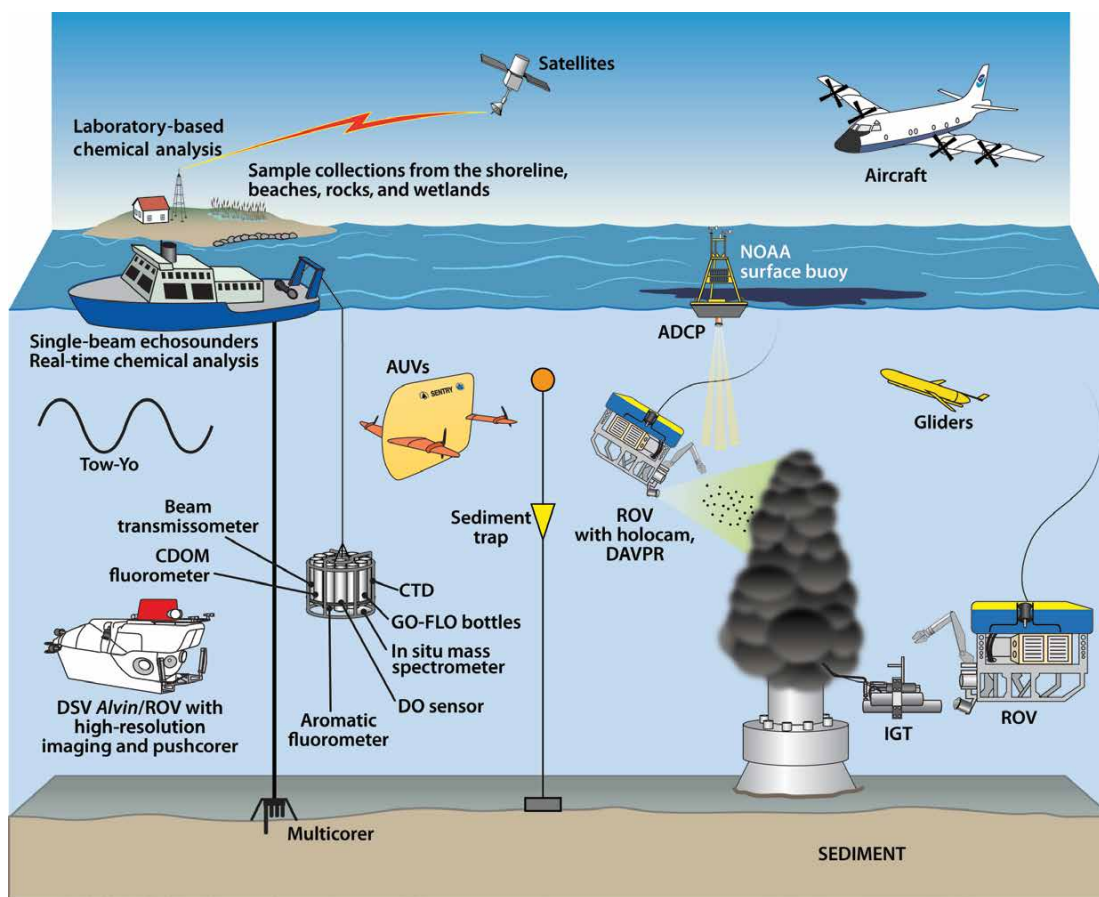

FIGURE 1. Vehicles, instrumentation and techniques used to detect oil following the Deepwater Horizon (DWH) oil spill. This includes satellites, aircraft, buoys (including an acoustic Doppler current profiler [ADCP]), and gliders. Sensors were placed on towed vehicles, rosettes, gliders, remotely operated vehicles (ROVs), and autonomous underwater vehicles (AUVs). These sensors included in situ membrane inlet mass spectrometers, aromatic and chromophoric dissolved organic matter (CDOM) fluorometers, a beam transmissometer, an in situ digital holographic camera (holocam), a digital autonomous video plankton recorder (DAVPR), dissolved oxygen (DO) sensors, conductivity-temperature-depth (CTD) packages, video, and cameras. Discrete samples were collected from the shoreline, the atmosphere (via aircraft and surface vessels), surface waters (via Teflon screens), subsurface waters (via GO-FLO bottles and sediment traps), and the seafloor. AUVs and ROVs collected samples directly from the leaking well with an isobaric gas-tight (IGT) sampler, and sediment samples were obtained via multicorer or pushcorer (not shown) by the ROVs and the deep submergence vehicle (DSV) *Alvin* in order to maintain the top millimeters of sediment where oil recently deposited from the DWH spill would be found. Real-time chemical analysis of oil onboard surface vessels as well as laboratory-based techniques are also shown. *Figure created by Jack Cook, Woods Hole Oceanographic Institution*

chromophoric dissolved organic matter, and beam transmissometers to detect suspended particulate matter. Digital holographic cameras (holocams) and particle size analyzers measured oil droplet size and distribution. Dissolved oxygen sensors, conductivity-temperature-depth (CTD) devices, and cameras were frequently included in sensor packages to collect data regarding the general characteristics of subsurface waters. Vessel-mounted single-beam echosounders were also employed to make acoustic observations to detect plumes of oil droplets and estimate the flow rate of the leaking oil (Weber et al., 2012). Discrete samples were collected from the atmosphere, surface waters, subsurface waters, and the seafloor. The different instruments used to detect oil have varying degrees of selectivity, sensitivity, and certainty. Quality assurance and quality control (QA/QC) for individual technologies also varied among academic laboratories, government institutions, and industry, as well as among different technologies. Additionally, each technology or instrument differs in cost, usability, and processing time (Table 1), all of which must be considered when determining how to best detect and monitor oil for future oil spill preparedness.

DETECTION OF SURFACE OIL

During the DWH spill, aerial reconnaissance flights were undertaken to assess the extent and magnitude of the surface oil using verbal reports and hand-held photography. As many as 20 fixed wing planes and 82 helicopters were deployed on a single day as part of the Unified Area Command (UAC) aerial asset fleet (US Coast Guard, 2011). Detection of surface oil by aerial observation is standard practice during spills for assessing spatial extent, estimating oil thickness, and determining the presence of oil that can be targeted for surface dispersant applications and for directing booming, skimming, and controlled burn operations (Lehr et al., 2010; Mabile, 2013). UAC's initial estimate for

the rate of discharge was approximately 1,000 barrels (bbl) d⁻¹, then amended to 5,000 bbl d⁻¹ based largely on aerial observations (1 bbl = 0.159 m³ or 159 liters). Independent analysts predicted rates as high as 27,500 bbl d⁻¹ based on these same results (Ramseur, 2010). This mismatch may have resulted from a discrepancy between the guidelines for estimating oil thickness on the basis of color and appearance (MacDonald, 2010). National Oceanic and Atmospheric Administration (NOAA) guidelines state that dark oil has an approximate thickness of 200 mm (NOAA Hazmat, 2012), while guidelines used by the UAC state the thickness for dark oil as approximately

2 mm (US Coast Guard, 2006). Accurate determination of the thickness of oil floating on water is technically challenging (Fingas and Brown, 2014), and constrains the precision of all remote-sensing estimates of surface oil quantity.

Surface oil was also appraised via space-based satellite remote sensing throughout the DWH spill. Responders were able to obtain satellite imagery at no cost through the International Charter for Space and Major Disasters (http://www.disasterscharter.org), and image acquisitions were made on every orbital pass throughout much of the spill. The northeastern GoM, where the surface oil was observed, encompasses 420,000 km² of
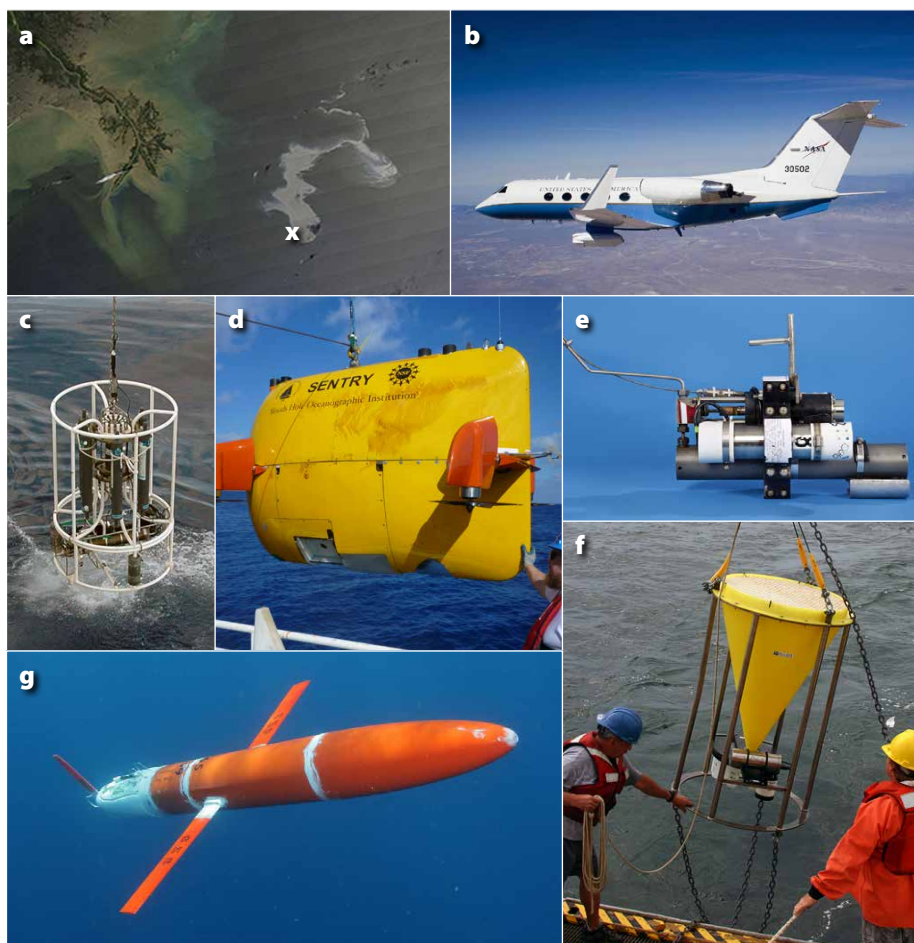

FIGURE 2. Examples of vehicles, instrumentation, and imagery used to detect oil following the Deepwater Horizon oil spill. (a) A satellite image of the oil slick with the location of the Macondo well shown by an "x" (*image courtesy of NASA*). (b) An uninhabited aerial vehicle synthetic aperture radar (UAVSAR) pod attached to a GulfStream III (*image courtesy of NASA*). (c) A rosette with CTD package, GO-FLO bottles, and a fluorometer (*photo by Robert Nelson, © WHOI*). (d) AUV *Sentry*, a 4 m long by 2 m high device that is particularly adept at mapping and can be equipped with numerous sensor packages (*photo by Cameron P. McIntyre, ©WHOI*). (e) An IGT sampler (*photo by Tom Kleindinst, ©WHOI*). (f) A funnel-shaped sediment trap (*photo by Matt Barton, ©WHOI*). (g) Spray, a seven-foot glider (*photo by Robert Todd, © WHOI*).

coastal ocean (i.e., within the US Exclusive Economic Zone), and it is likely that no previous oceanic event has had such sustained and intensive satellite observation over a similar area. Satellite remote-sensing instruments include passive sensors, which image the ocean in visible color or multispectral bandwidths, and microwave sensors, which transmit radar energy and quantify the return of that energy from the ocean surface, with the latter used more commonly for oil spill applications. All passive sensors are constrained by cloud cover, and ocean color sensors often require appropriate sun angles to be effective (Leifer et al., 2012). Passive ocean color sensors—including modern and medium resolution imaging spectroradiometers—provided information on the spill's spatial extent using sensitivity to the bright sun glint signature that oil slicks generate (Hu et al., 2011, and see Figure 2a). The Hyperspectral Imager for the Coastal Ocean sensor aboard the International Space Station also provided coverage. Microwave sensors, such as satellite-borne synthetic aperture radar (SAR) instruments, are not constrained by available light or cloud cover and offer unobstructed views of spills. These sensors acquired a total of 452 SAR images of the northeastern GoM during the spill (Garcia-Pineda et al., 2013). Imaging radar instruments were also used and, like SAR, rely upon detection of the back-scatter contrast between the floating oil and the sea surface without oil. They can be effective under all sky conditions (Leifer et al., 2012), but require light to moderate winds for effective contrasts (Brekke and Solberg, 2005). All space-based sensors increase the spatial and temporal coverage of oil spills, though SAR has fine spatial resolution over a smaller footprint and passive sensors have lower resolution over a larger footprint. Ocean color sensors complement SAR coverage by offering advantages for differentiating oil from false positives (e.g., *Sargassum*, *Trichodesmium*, debris) using numerous spectral bands and the potential to estimate oil volume.

Additional airborne remote-sensing assets were mobilized by NASA, NOAA, and the US Geological Survey, including UAVSAR (uninhabited aerial vehicle synthetic aperture radar; see Figure 2b) and AVIRIS (Airborne Visible/Infrared Imaging Spectrometer; Clark et al., 2010; Minchew et al., 2012). The AVIRIS sensor, deployed on a high-altitude NASA ER-2 aircraft, extensively measured the region affected by the spill during 11 flights conducted between May 6 and May 25, 2010. In total, AVIRIS measured more than 100,000 km^2 (38,610 square miles) aboard a NASA ER-2 aircraft. Results from AVIRIS quantified the extent of oiling in portions of the marsh vegetation canopy of Barataria Bay, Louisiana (Kokaly et al., 2013), and also refined estimates for thickness classes for

TABLE 1. Properties of in situ sensors and laboratory-based instruments used to detect and characterize oil-derived compounds in the Gulf of Mexico following the Deepwater Horizon oil spill.

	Instrument	Analyte(s)	Selectivity	Certainty	Sensitivity	Cost ($)	Speed	Usability	Availability
IN SITU	Inlet mass spectrometer	C_1-C_4 hydrocarbons, benzene, naphthalene	High	High	High	160 K	Immediate	Specialized	Limited
	Fluorometer	CDOM[a] and aromatic hydrocarbons	Low	High	High	6–13 K	Immediate	Non-expert	Wide
	Beam transmissometer	Water column particulate matter	Low	High	High	7–8 K	Immediate	Non-expert	Wide
	Holocam	Oil droplets	High	High	High	Unavailable	Immediate	Specialized	Limited
LABORATORY BASED	GC-FID[b]	C_8-C_{40} hydrocarbons	High	High	High	~50 K	Weeks	Specialized	Wide
	GC-MS[c]	C_8-C_{40} hydrocarbons	High	High	High	70–100 K	Weeks	Specialized	Wide
	GC-MS in SIM[d] mode	C_8-C_{40} hydrocarbons	High	High	Highest	70–100 K	Weeks	Specialized	Wide
	GC×GC-FID[e]	C_8-C_{40} hydrocarbons	Highest	Highest	High	~100 K	Months	Specialized	Limited
	GC×GC-TOF-MS[f]	C_8-C_{40} hydrocarbons	Highest	Highest	High	~250 K	Months	Specialized	Limited
	FT-IR[g]	Bulk oil	Average	Average	< Average	15–20 K	Days	Specialized	Wide
	FT-ICR-MS[h]	Hydrocarbons, oxidized hydrocarbons, and polar (N,S,O-containing compounds)	Highest	High	Highest	1–2 M	Months	Specialized	Limited
	TLC-FID[i]	Fractions of oil separated by polarity	Average	Highest	Average	50–60 K	Days	Non-expert	Wide
	GC-irm-MS[j]	Stable carbon and hydrogen isotopic composition of oil compounds	Highest	Highest	Highest	~300 K	Weeks	Specialized	Limited
	AMS[k]	^{14}C composition of oil and oil compounds	Highest	Highest	Highest	2–3 M	Months	Specialized	Limited
	Ramped pyrolysis	Fractions of oil separated by thermochemical stability	Average	High	Average	65 K	Weeks	Specialized	Limited

[a] CDOM: chromophoric dissolved organic matter. [b] GC-FID: gas chromatography coupled to flame ionization detection. [c] GC-MS: gas chromatography coupled to mass spectrometer. [d] SIM: selected ion monitoring. [e] GC×GC-FID: comprehensive two-dimensional gas chromatography (GC×GC) coupled to flame ionization detection. [f] GC×GC-TOF-MS: GC×GC coupled to a time-of-flight mass spectrometer. [g] FT-IR: Fourier transform infrared spectroscopy. [h] FT-ICR-MS: Ultrahigh resolution Fourier transform ion cyclotron resonance mass spectrometer. [i] TLC-FID: thin layer chromatography–flame ionization detection. [j] GC-irm-MS: gas chromatography-isotope ratio monitoring-mass spectrometry. [k] AMS: accelerator mass spectrometer.

surface oil based on the shape of near-infrared absorption features (Clark et al., 2010). The UAVSAR instrument was deployed over the spill area between June 2010 and July 2012 and used to characterize the oil within a slick, distinguishing very thin film (~1 mm) oil sheens from thicker (~100 mm) oil emulsions (Minchew et al., 2012).

To detect oil that reached the surface and evaporated into the atmosphere, a NOAA chemically instrumented P-3 aircraft was used for the first time following an oil spill. Atmospheric plumes of volatile hydrocarbons containing one to 11 carbon atoms were recorded on survey flights taken on June 8 and 10, 2010, and were calculated to come from a surface source area of ~2 km^2 immediately adjacent to the spill. The aerial extents of these plumes were used, along with surface and subsurface chemical measurements, to determine the flow rate and distribution of the oil in the environment (Ryerson et al., 2011, 2012). Petroleum hydrocarbons detected in atmospheric samples were also collected aboard three surface vessels: F/V *Eugenie*, R/V *Pelican*, and R/V *Thomas Jefferson*. These samples and additional whole air samples

taken during the P-3 survey flights were later analyzed via gas chromatography in research laboratories. The EPA Airborne Spectral Photometric Environmental Collection Technology monitoring system was deployed during in situ burn operations of oil and collected data regarding particulate and combustion products (Kroutil et al., 2010).

The high rate of image acquisition and large areas of interest covered by remote sensing challenged the ability of responders to segment images into regions of oil-covered water and clean sea. Throughout the spill, the NOAA National Environmental Satellite, Data, and Information Service posted daily interpretations and predictions regarding the extent of surface oil and its movement. In addition, much was learned by post-emergency analysis of remote-sensing data and development of semi-automated procedures for detection of floating oil. The Texture Classifying Neural Network algorithm, which uses expert training sets to segment oil-covered water, and the Oil Emulsion Detection Algorithm, which detects radar absorption contrasts caused by thick oil and oil-water emulsions, were refined for use with DWH SAR imagery

based on analysis of 172 separate images (Garcia-Pineda et al., 2013). Data from AVIRIS have been analyzed at scales similar to spectroradiometer images (300 m resolution) to improve slick detection and slick thickness classifications for ocean color sensors (Sun et al., 2015). A comprehensive treatment of surface oil detections by SAR compared the DWH surface oil to natural oil slicks throughout the GoM and produced a series of 12-hour interpolations of DWH surface oil volumes over ocean area (m^3 km^{-2}) between April 24 and August 3, 2010 (MacDonald et al., 2015). These results indicate that the DWH surface oil produced a footprint vastly different from background seepage. The floating oil covered a patchy, amorphous region that changed constantly under the influence of surface currents and wind. The volume of oil detected by SAR was gridded across an array of 5 km × 5 km cells; when averaged over the period April 24 (first SAR image) to August 3 (no oil detected), the surface oil detected by SAR covered an area of 11,804 km^2, with a volume of 22,619 m^3 (Figure 3). Remote-sensing information helped reach the conclusion that response operations,
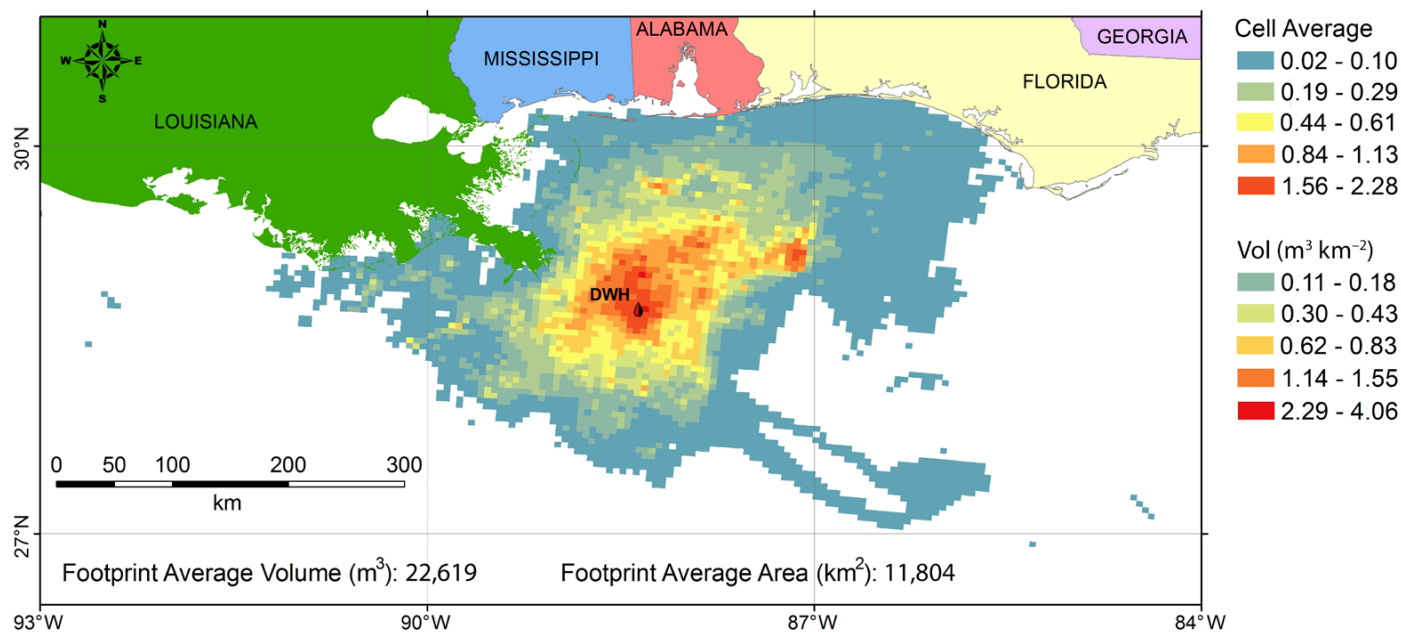

FIGURE 3. Synthetic aperture radar (SAR) detection of surface oil from Deepwater Horizon. Distribution and average volume of surface oil (m^3 km^{-2}) from DWH discharge is gridded at a 5 km × 5 km scale across a cumulative footprint of 149,000 km^2. Average values are calculated from a 12-hour regular time series of this grid for April 24–August 3, 2010. *From MacDonald et al. (2015)*

particularly subsurface application of dispersants, reduced surface oil volume by 21%, while increasing the area over which the remaining oil was distributed by 49% (MacDonald et al., 2015).

DETECTION OF SUBSURFACE OIL

CTD rosette profilers (example shown in Figure 2c) equipped with fluorometers, transmissometers, and dissolved oxygen sensors were most commonly used to detect DWH subsurface oil, obtain hydrographic profiles, and collect water samples (Diercks et al., 2010; Joye et al., 2011; Wade et al., 2011; Reddy et al., 2012; Zhou et al., 2013; Bianchi et al., 2014). Dissolved oxygen concentrations were measured within plumes to detect hypoxic conditions resulting from oil biodegradation. The reduction in dissolved oxygen proved to be an excellent proxy tracer for oil (Du and Kessler, 2012). Real-time fluorescence monitoring provided a sensitive method for detecting aromatic hydrocarbons in the water column, validating oil dispersion. Discrete water samples analyzed by gas chromatography confirmed that the subsurface fluorescence maxima were due to the presence of oil. To this end, a variety of in situ fluorometers were deployed during the DWH oil spill, including the Chelsea Technologies Group AQUAtracka, the Turner Designs Cyclops, and Sea-Bird Scientific's Environmental Characterization Optics (ECO) instrument. Fluorometer performance testing was subsequently conducted in a wave tank to validate the DWH field data, provide intercomparability among sensors, and demonstrate that estimates of oil concentration could be obtained via fluorescence measurements with reasonable accuracy (Conmy et al., 2014). Results improved confidence in the ability to compare data acquired by ECO, taken early in the spill when there were relatively high concentrations of oil, with those acquired with AQUAtracka, taken later in the spill when oil concentrations were lower.

Historically, fluorescence has been used to detect oil dispersion from surface slicks down into the water column during spills as per the Special Monitoring of Applied Response Technologies protocols (SMART, 2006). Fluorescence sensors detected and tracked the presence of oil, but could not provide information on the degree of dispersion because oil was released directly into the water column. For this, particle size analysis of the droplet size distribution is needed to confirm physical (droplets > ~70 mm) or chemically enhanced (< ~70 mm) oil dispersion (Lunel, 1993). Sensors used included a beam transmissometer (the Sequoia LISST, Laser In-situ Scattering and Transmissometry) and the holocam, a small, low power plankton imaging system not originally intended for oil spills (Loomis et al., 2007). The holocam was mounted on an ROV to collect images and measurements of oil droplets that were distinguished from plankton via this method (Loomis, 2011; Figure 4). The resolution of the holocam was sufficient to identify oil droplets down to a size of ~30 microns. Knowledge of the droplet size distribution and particle type during a spill is critical for determining how fast droplets will rise and ultimately how the oil will be transported.

Although many vertical profiles were collected (>14,000; Joint Analysis Group, 2012), profiling casts are time-intensive, and transit time between stations causes sampling time to be lost. Thus, coarse coverage through space and time was an issue. To circumvent this limitation, sampling efforts were enhanced by combining vertical profiling via CTD casts and tow-yo sled (a towed undulating platform) runs with long-range surveys by the AUV *Sentry* (Figure 2d) between 1,030 m and 1,300 m depth in May and June 2010. Water column samples collected using the vertical rosette profiler (Figure 2c) confirmed the presence of oil-derived compounds
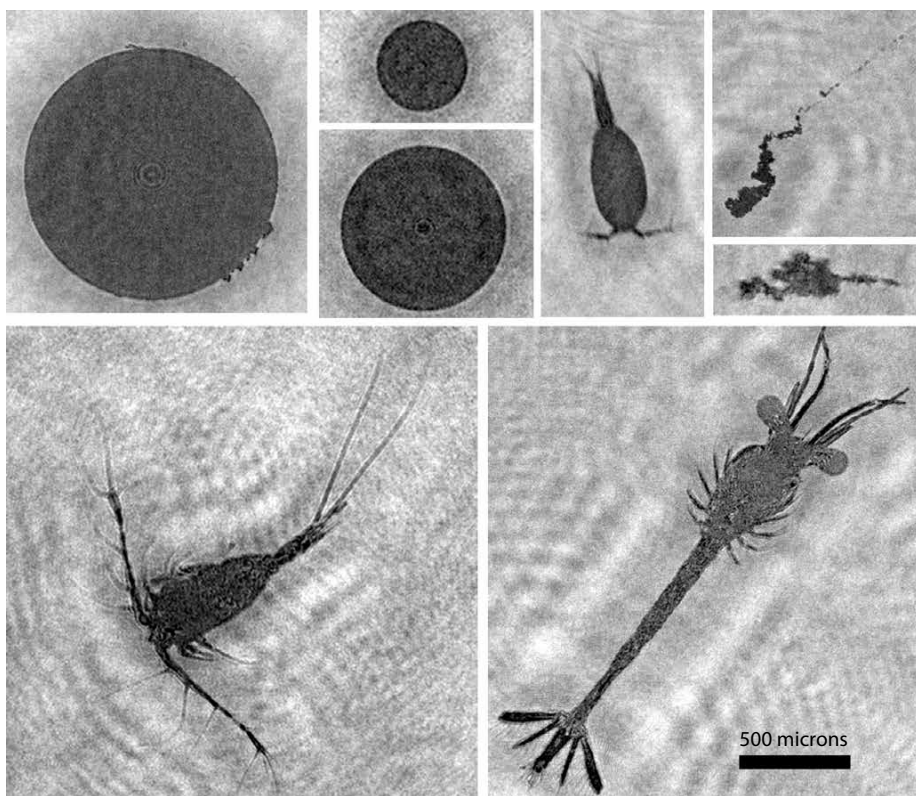

FIGURE 4. Holographic images from the Gulf of Mexico. Clockwise from upper left: Three oil droplets, a cyclopoid copepod, two marine snow particles, a decapod larva, and a calanoid copepod. The scale bar is 500 microns and applies to all images. *Courtesy of Cabell Davis, Woods Hole Oceanographic Institution*

in plumes, which was later verified via laboratory GC analysis (Camilli et al., 2010). Sensors attached to the profiler included an in situ membrane inlet mass spectrometer, a dissolved oxygen sensor, and two fluorometers (Seapoint SUVF and Chelsea Technologies Group AQUAtracka). The AUV *Sentry* was also equipped with an in situ membrane inlet mass spectrometer and performed three long-range surveys that covered a total distance of 235 km. The subsurface plumes of oil detected by these methods were consistent with findings from an earlier AUV survey conducted by the AUV *Dorado* operated by Monterey Bay Aquarium Research Institute (MBARI) on June 2 and 3, 2010, ~10 km southwest of the well site (Camilli et al., 2010, and references therein).

DETERMINING THE CHEMICAL AND CARBON ISOTOPIC COMPOSITION OF OIL

Oil from the DWH spill was documented along thousands of kilometers of shoreline in the northern GoM (Nixon et al., 2016), including in coastal waters (Allan et al., 2012), on beaches (e.g., Aeppli et al., 2012) and rocks (Radović et al., 2014), and in wetlands of the Mississippi River Delta ecosystem (e.g., Mendelssohn et al., 2012; Overton et al., 2014). Oil was also collected from surface water using Teflon screens (Aeppli et al., 2013). Analysis of its specific chemical composition was essential for determining if it originated from the DWH oil spill and, if so, how it was being altered over time. Oil is comprised of thousands of different compounds with varying physicochemical properties that interact differently with biological and physical processes in the environment. These processes are collectively known as "weathering" and bring about changes in the chemical composition and physical characteristics of oil. Examination of the specific chemical compounds present in oil that persist in the environment can provide insight into weathering processes. Typically, oil-containing samples are solvent-extracted to isolate oil compounds prior to analysis via gas chromatography, which employs a high-resolution capillary column coupled to either flame ionization detection or a mass spectrometer (GC-FID or GC–MS). GC-FID enables quantification of GC-amenable compounds whereas a mass spectrometer provides structural information in addition to quantification of oil-derived compounds. Comprehensive two-dimensional gas chromatography (GC×GC) can be used to resolve an order of magnitude more compounds from complex mixtures such as oil. Coupled to either FID or a time-of-flight mass spectrometer (TOF-MS), GC×GC is able to resolve biomarker compounds that can then be used to determine the oil's source (Nelson et al., 2016). Many compounds present in oil may not be GC amenable, however, and this limitation has been shown to increase with weathering (Aeppli et al., 2012). Ultrahigh resolution Fourier transform ion cyclotron resonance mass spectrometry (FT-ICR-MS) can be used to obtain information about oil compounds that have been oxidized by weathering as well as any polar components of oil present in the original oil (McKenna et al., 2013; Ruddy et al., 2014). Oil collected directly from the leaking well with an isobaric gas-tight sampler (see Figure 2e) by the ROV *Millennium 42* was examined for its specific oil and gas composition via GC-FID, GC-MS, GC×GC-FID, and GC×GC-TOF-MS (Reddy et al., 2012), as well as FT-ICR-MS (McKenna et al., 2013). These analyses provided detailed compositional and quantitative data on the gas and oil that flowed from the well, in particular, that the gas-to-oil ratio of the fluids flowing from the well was 1,600 standard cubic feet per petroleum barrel (Reddy et al., 2012).

Techniques that utilize GC-MS and GC-FID to analyze oil are well established and have QA/QC protocols associated with them. FT-ICR-MS and GC×GC are, however, more specialized and less established, and the analyses are more time consuming and expensive (see Tarr et al., 2016, in this issue for further details). Multiple samples can take weeks to months of processing before data with the appropriate QA/QC can be provided. The DWH efforts have resulted in more rapid throughput times for FT-ICR-MS and GC×GC techniques and refined targeting of compounds present in oil.

Lab techniques for determining the bulk properties of oil take less time and can provide useful information regarding the chemical composition of oil. A study by Aeppli et al. (2012) details the weathering of oil in oil-soaked sand patties originating from the DWH spill and collected from GoM beaches. These authors describe the oxidation of oil in the environment utilizing GC-FID to detect and quantify weathered oil; thin layer chromatography-flame ionization detection to quantify the relative abundance of saturated, aromatic, and oxygenated fractions of oil; Fourier transform infrared spectroscopy (FT–IR) to reveal the carboxylation and hydroxylation of oil; and elemental analysis to determine changes in the oxygen content of oil over time. These bulk studies were followed up by FT-ICR-MS approaches to further examine oxygen-containing oil-derived compounds (Ruddy et al., 2014).

Analysis of the carbon isotopic composition of oil can be employed to determine its presence in more complex samples. Together with hydrogen isotopic composition (δD), stable carbon isotope composition ($\delta^{13}C$) was examined for the reservoir fluid from the well (Reddy et al., 2012). These data informed subsequent studies, including how oil was incorporated into the plankton food web, which was determined by examining $\delta^{13}C$ of oil and two plankton class sizes (Graham et al., 2010). Phytoplankton and suspended particulates examined were depleted in ^{13}C because they had incorporated oil. Oil contains no radiocarbon (^{14}C) due to its age, and as such, the depletion of natural abundance radiocarbon ($\Delta^{14}C$) in samples can be used as an inverse tracer of oil (e.g., White et al., 2008). Compared to $\delta^{13}C$, $\Delta^{14}C$ has a

larger dynamic range of values. Biological uptake of carbon derived from oil was confirmed by additional analysis of the Δ^{14}C of plankton (Chanton et al., 2012) and that of fish tissue, invertebrate tissue, and shell samples (Wilson et al., 2015), which were all depleted in ^{14}C due to the incorporation of oil. This approach was also used to examine microbial phospholipid fatty acids in impacted marsh sediments, revealing that oil-derived carbon

collected both sediment and coral samples (White et al., 2012). These samples were analyzed in various laboratories to determine their chemical compositions and, in some instances, natural ^{14}C abundance (see Passow and Ziervogel, 2016, in this issue for further details).

Both the chemical and carbon isotopic composition of oil was used to provide estimates of the flux of oil from the DWH spill to the seafloor. The Δ^{14}C com-

spectroscopy, and GC-MS) to newer techniques that are less established, yet provide much greater certainty (e.g., GC×GC and FT-ICR-MS). There is a need to establish QA/QC for all methods applied. Data produced by the NRDA and BP met rigorous QA/QC standards. In addition, the National Institute of Standards and Technology (NIST) ran intercalibration exercises for oil and sediments and made available standard reference material for the oil released in the DWH spill. In 2015, The Gulf of Mexico Research Initiative inaugurated the hydrocarbon intercalibration exercise to ensure that valid and comparable data are produced to the academic community. Twenty laboratories participated and analyzed the NIST standard reference material oil. Contributed results included analyses of traditional petroleum hydrocarbons (alkanes, aromatics, and hopane, and sterane biomarkers), toxicity, viscosity, and FT-ICR-MS (nontraditional) (Murray et al., 2016).

> " The DWH spill enabled scientists to demonstrate the reliability of many new technologies, but to be effective, these techniques must be implemented with appropriate transfer of technology from government, academia, and industry to responders. "

was incorporated into microbial biomass (Mahmoudi et al., 2013). In addition to studies determining the biological incorporation of oil, examination of the δ^{13}C and Δ^{14}C of marsh sediments contaminated by the DWH spill described the presence and quantity of oil in relation to the thermochemical stability of different sedimentary organic carbon pools (Pendergraft et al., 2013). Δ^{14}C also provided insight into the transformation of oil compounds in the environment, indicating that even as oil is weathered, it remains devoid of ^{14}C and does not incorporate recent photosynthetic material (Aeppli et al., 2012).

Oil that had transited through the water column to the seafloor was collected by funnel-shaped sediment traps (see Figure 2f), and discrete sediment samples were obtained from surface vessels using grab samplers (Liu et al., 2012) or multicorers (Montagna et al., 2013; Valentine et al., 2014; Chanton et al., 2015). ROVs collected sediment push cores from the seafloor, and DSV *Alvin*

position of surface sediments was used to indicate the presence of oil, which is depleted relative to contemporary sedimentary organic matter. Analysis of the bulk isotopic properties of sediment is less specific than analysis of the aforementioned compound class or of weathered oil (previously described by Aeppli et al., 2012); however, this approach provided a conservative estimate that 0.5%–9.1% of the released oil was deposited on the seafloor (Chanton et al., 2015). A more specific estimate was made using chemical distributions of oil-derived compounds in surface sediments, with specific attention to the concentration of a recalcitrant biomarker of crude oil, 17α,21β-hopane, indicating that 1.8%–14.4% of the released oil was present in the surface sediments (Valentine et al., 2014).

Methods to determine the composition of oil and how it is weathered in the environment vary from more established approaches that are decades old (e.g., bulk oxygen, ^{14}C analysis, infrared

CONCLUSIONS

Through a combination of established and new technologies, the toolbox for responding to an oil spill of the magnitude of the DWH spill has expanded. The majority of vehicles, instruments, and techniques described here were used extensively prior to the DWH oil spill to address questions related to general oceanographic research. Some were novel to oil spills, including the chemically instrumented P-3 aircraft (Ryerson et al., 2012); the AUV *Sentry* (Camilli et al., 2010); the isobaric gas-tight sampler (Reddy et al., 2012); the holocam (Davis and Loomis, 2014); and the detection of dispersant components (Kujawinski et al., 2011); all of these were developed with government funding to address basic scientific questions. Further, the in situ mass spectrometer (Camilli et al., 2010) was a new concept for researchers and oil responders alike. The resourcefulness of scientists and the extended time period of the spill enabled the successful application of

these technologies, which both improve our understanding of the fate of oil in the environment and expand our capacity to detect oil.

It is now the responsibility of the scientific and response communities to critically examine these technologies to assess their future utility in both large- and small-scale spills. In particular, QA/QC criteria must be developed for all instruments and analyses so that accuracy and precision are well defined, and methods can be repeated by multiple users. It is important to evaluate the percentage of time these real-time (or quasi real-time) measurements are correct and whether this is sufficient to inform future response or damage assessment decisions. In addition, the perception that discrete sample results are the "gold" standard and have reduced error is incorrect. Discrete samples and satellite remote sensing provide two different types of spatial and temporal measures; their value could be greatly leveraged by coordinated collection of discrete samples that are taken synoptically with satellite observations. The dispersed and highly patchy nature of surface oil can produce very different information regarding oil thickness, for example, for closely spaced collections. Remote-sensing data provide a means to generalize from discrete samples, but is difficult when satellite returns are not calibrated against known standards. Although measuring the thickness of floating oil layers is inherently challenging, better attention to careful documentation of surface oil characteristics could improve the interpretation of satellite sensors. Robust and reliable methods must be established for in situ and remote sensing techniques, and these in turn should be compared to data determined from discrete samples from the DWH spill so that any discrepancies in quantity and chemical and physical composition of oil can be determined. The advantages of real-time (or quasi-real-time) measurements go beyond their quick turn-around time for results; an in situ mass spectrometer, for example, may provide more accurate information on volatile components of oil present in the water column than grab bottle samples, which may be compromised when collected. Additionally, in situ fluorescence and mass spectrometry offer advantages in monitoring over obtaining grab bottle samples that span relatively small areas of water column. As a science and response community, it is essential to understand and define trade-offs between accuracy and precision, and between different temporal-spatial techniques. The balance between the two is not new and is irrespective of the target analyte.

The DWH spill enabled scientists to demonstrate the reliability of many new technologies, but to be effective, these techniques must be implemented with appropriate transfer of technology from government, academia, and industry to responders. In addition, specific improvements to oil spill response should include (1) greater collection of surface samples for chemical and physical analyses; (2) better characterization of surface oil samples so that the interpretation of satellite data can be improved; (3) improved spatial, temporal, and spectral resolution for satellites; (4) longer sampling and duration of analysis for unmanned vehicles; and (5) the availability and correct outfitting of ships with hydrographic equipment composed of real-time, two-way cabled CTD rosettes capable of full ocean depth sampling with, at a minimum, dissolved oxygen sensors, hydrocarbon (not pigment) fluorometers, and transmissometers, as well as particle size analyzers, if possible. The availability of assets leveraged in response to the DWH spill was impressive, and from a logistical perspective, occurred in an easily accessible region. No matter where future spills occur, it is imperative that the spill and scientific communities know what information technologies could provide. This knowledge is necessary for taking a multipronged approach to detecting oil, including a comprehensive sampling and collection program that will inform the response, damage assessment, and fundamental science of a spill. ℞

REFERENCES

Aeppli, C., C.A. Carmichael, R.K. Nelson, K.L. Lemkau, W.M. Graham, M.C. Redmond, D.L. Valentine, and C.M. Reddy. 2012. Oil weathering after the Deepwater Horizon disaster led to the formation of oxygenated residues. *Environmental Science & Technology* 46(16):8,799–8,807, http://dx.doi.org/10.1021/es3015138.

Aeppli, C., C.M. Reddy, R.K. Nelson, M.Y. Kellermann, and D.L. Valentine. 2013. Recurrent oil sheens at the Deepwater Horizon disaster site fingerprinted with synthetic hydrocarbon drilling fluids. *Environmental Science & Technology* 47(15):8,211–8,219, http://dx.doi.org/10.1021/es4024139.

Allan, S.E., B.W. Smith, and K.A. Anderson. 2012. Impact of the Deepwater Horizon oil spill on bioavailable polycyclic aromatic hydrocarbons in Gulf of Mexico coastal waters. *Environmental Science & Technology* 46(4):2,033–2,039, http://dx.doi.org/10.1021/es202942q.

Bianchi, T.S., C. Osburn, M.R. Shields, S. Yvon-Lewis, J. Young, L. Guo, and Z. Zhou. 2014. Deepwater Horizon oil in Gulf of Mexico waters after 2 years: Transformation into the dissolved organic matter pool. *Environmental Science & Technology* 48(16):9,288–9,297, http://dx.doi.org/10.1021/es501547b.

Boehm, P.D., K.J. Murray, and L.L. Cook. 2016. Distribution and attenuation of polycyclic aromatic hydrocarbons in Gulf of Mexico seawater from the Deepwater Horizon oil accident. *Environmental Science & Technology* 50:584–592, http://dx.doi.org/10.1021/acs.est.5b03616.

Brekke, C., and A.H.S. Solberg. 2005. Oil spill detection by satellite remote sensing. *Remote Sensing of Environment* 95(1):1–13, http://dx.doi.org/10.1016/j.rse.2004.11.015.

Camilli, R., C.M. Reddy, D.R. Yoerger, B.A. Van Mooy, M.V. Jakuba, J.C. Kinsey, C.P. McIntyre, S.P. Sylva, and J.V. Maloney. 2010. Tracking hydrocarbon plume transport and biodegradation at Deepwater Horizon. *Science* 330:201–204, http://dx.doi.org/10.1126/science.1195223.

Chanton, J.P., J. Cherrier, R.M. Wilson, J. Sarkodee-Adoo, S. Bosman, A. Mickle, and W.M. Graham. 2012. Radiocarbon evidence that carbon from the Deepwater Horizon spill entered the planktonic food web of the Gulf of Mexico. *Environmental Research Letters* 7(4):045303, http://dx.doi.org/10.1088/1748-9326/7/4/045303.

Chanton, J., T. Zhao, B.E. Rosenheim, S. Joye, S. Bosman, C. Brunner, K.M. Yeager, A.R. Diercks, and D. Hollander. 2015. Using natural abundance radiocarbon to trace the flux of petro-carbon to the seafloor following the Deepwater Horizon oil spill. *Environmental Science & Technology* 49(2):847–854, http://dx.doi.org/10.1021/es5046524.

Clark, R.N., G.A. Swayze, I. Leifer, K.E. Livo, R. Kokaly, T. Hoefen, S. Lundeen, M. Eastwood, R.O. Green, N. Pearson, and others. 2010. A method for quantitative mapping of thick oil spills using imaging spectroscopy. *US Geological Survey Open-File Report 2010-1167*, 51 pp.

Conmy, R.N., P.G. Coble, J. Farr, A.M. Wood, K. Lee, W.S. Pegau, I.D. Walsh, C.R. Koch, M.I. Abercrombie, M.S. Miles, and others. 2014. Submersible optical sensors exposed to chemically dispersed crude oil: Wave tank simulations for improved oil spill monitoring. *Environmental Science & Technology* 48(3):1,803–1,810, http://dx.doi.org/10.1021/es404206y.

Davis, C.S., and N.C. Loomis. 2014. NRDA Image Data Processing Plan—Holocam: Data Processing Methods. DWH-AR0047462.

Diercks, A.R., R.C. Highsmith, V.L. Asper, D. Joung, Z. Zhou, L. Guo, A.M. Shiller, S.B. Joye, A.P. Teske, N. Guinasso, and T.L. Wade. 2010. Characterization of subsurface polycyclic aromatic hydrocarbons at the Deepwater Horizon site. *Geophysical Research Letters* 37, L20602, http://dx.doi.org/10.1029/2010GL045046.

Du, M., and J.D. Kessler. 2012. Assessment of the spatial and temporal variability of bulk hydrocarbon respiration following the Deepwater Horizon oil spill. *Environmental Science & Technology* 46(19):10,499–10,507, http://dx.doi.org/10.1021/es301363k.

Fingas, M., and C. Brown. 2014. Review of oil spill remote sensing. *Marine Pollution Bulletin* 83(1):9–23, http://dx.doi.org/10.1016/j.marpolbul.2014.03.059.

Garcia-Pineda, O., I. MacDonald, X. Li, C. Svejkovsky, M. Hess, D. Dukhovskoy, and S.L. Morey. 2013. Detection of floating oil anomalies from the Deepwater Horizon oil spill with synthetic aperture radar. *Oceanography* 26(2):124–137, http://dx.doi.org/10.5670/oceanog.2013.38.

Graham, W.M., R.H. Condon, R.H. Carmichael, I. D'Ambra, H.K. Patterson, L.J. Linn, and F.J. Hernandez Jr. 2010. Oil carbon entered the coastal planktonic food web during the Deepwater Horizon oil spill. *Environmental Research Letters* 5(4):045301, http://dx.doi.org/10.1088/1748-9326/5/4/045301.

Hu, C., R.H. Weisberg, Y. Liu, L. Zheng, K.L. Daly, D.C. English, J. Zhao, and G.A. Vargo. 2011. Did the northeastern Gulf of Mexico become greener after the Deepwater Horizon oil spill? *Geophysical Research Letters* 38, L09601, http://dx.doi.org/10.1029/2011GL047184.

Joint Analysis Group, Deepwater Horizon Oil Spill. 2012. *Review of Subsurface Dispersed Oil and Oxygen Levels Associated with the Deepwater Horizon MC252 Spill of National Significance.* NOAA Technical Report NOS OR&R 27, National Oceanic and Atmospheric Administration, US Department of Commerce, Washington, DC, 93 pp., https://repository.library.noaa.gov/view/noaa/390.

Joye, S.B., I.R. MacDonald, I. Leifer, and V. Asper. 2011. Magnitude and oxidation potential of hydrocarbon gases released from the BP oil well blowout. *Nature Geoscience* 4(3):160–164, http://dx.doi.org/10.1038/ngeo1067.

Kokaly, R.F., B.R. Couvillion, J.M. Holloway, D.A. Roberts, S.L. Ustin, S.H. Peterson, S. Khanna, and S.C. Piazza. 2013. Spectroscopic remote sensing of the distribution and persistence of oil from the Deepwater Horizon spill in Barataria Bay marshes. *Remote Sensing of Environment* 129:210–230, http://dx.doi.org/10.1016/j.rse.2012.10.028.

Kroutil, R.T., S.S. Shen, P.E. Lewis, D.P. Miller, J. Cardarelli, M. Thomas, T. Curry, and P. Kudaraskus. 2010. Airborne remote sensing for Deepwater Horizon oil spill emergency response. *SPIE (international society for optics and photonics) Proceedings, vol. 7812, Imaging Spectrometry XV*, S.S. Shen and P.E. Lewis, eds, http://dx.doi.org/10.1117/12.863258.

Kujawinski, E.B., M.C. Kido Soule, D.L. Valentine, A.K. Boysen, K. Longnecker, and M.C. Redmond. 2011. Fate of dispersants associated with the Deepwater Horizon oil spill. *Environmental Science & Technology* 45(4):1,298–1,306, http://dx.doi.org/10.1021/es103838p.

Lehr, W., S. Bristol, and A. Possolo. 2010. *Oil Budget Calculator: Deepwater Horizon Technical Documentation*. The Federal Interagency Solutions Group, 217 pp., http://www.restorethegulf.gov/sites/default/files/documents/pdf/OilBudgetCalc_Full_HQ-Print_111110.pdf.

Leifer, I., W.J. Lehr, D. Simecek-Beatty, E. Bradley, R. Clark, P. Dennison, Y. Hu, S. Matheson, C.E. Jones, B. Holt, and M. Reif. 2012. State of the art satellite and airborne marine oil spill remote sensing: Application to the BP Deepwater Horizon oil spill. *Remote Sensing of Environment* 124:185–209, http://dx.doi.org/10.1016/j.rse.2012.03.024.

Liu, Z., J. Liu, Q. Zhu, and W. Wu. 2012. The weathering of oil after the Deepwater Horizon oil spill: Insights from the chemical composition of the oil from the sea surface, salt marshes and sediments. *Environmental Research Letters* 7(3):035302, http://dx.doi.org/10.1088/1748-9326/7/3/035302.

Loomis, N. 2011. *Computational Imaging and Automated Identification for Aqueous Environments*. PhD Thesis, MIT/WHOI Joint Program.

Loomis, N., J. Dominguez-Caballero, W. Li, C. Hu, C. Davis, J. Milgram, and G. Barbastathis. 2007. A compact, low-power digital holographic imaging system for automated plankton taxonomical classification. Paper presented at the Fourth International Zooplankton Production Symposium–Human and Climate Forcing of Zooplankton Populations, May 28–June 1, 2007, Hiroshima, Japan.

Lunel, T. 1993. Dispersion: Oil droplet size measurements at sea. Pp. 794–795 in *Report of the 1993 International Oil Spill Conference: Prevention, Preparedness, Response,* http://dx.doi.org/10.7901/2169-3358-1993-1-794.

Mabile, N.J. 2013. Considerations for the application of controlled in-situ burning. *Oil and Gas Facilities* 2(02):72–84, http://dx.doi.org/10.2118/157602-PA.

MacDonald, I.R. 2010. Deepwater disaster: How the oil spill estimates got it wrong. *Significance* 7(4):149–154, http://dx.doi.org/10.1111/j.1740-9713.2010.00449.x.

MacDonald, I.R., O. Garcia-Pineda, A. Beet, S. Daneshgar Asl, L. Feng, G. Graettinger, D. French-McCay, J. Holmes, C. Hu, F. Huffer, and others. 2015. Natural and unnatural oil slicks in the Gulf of Mexico. *Journal of Geophysical Research* 120:8,364–8,380, http://dx.doi.org/10.1002/2015JC011062.

Mahmoudi, N., T.M. Porter, A.R. Zimmerman, R.R. Fulthorpe, G.N. Kasozi, B.R. Silliman, and G.F. Slater. 2013. Rapid degradation of *Deepwater Horizon* spilled oil by indigenous microbial communities in Louisiana salt-marsh sediments. *Environmental Science & Technology* 47(23):13,303–13,312, http://dx.doi.org/10.1021/es4036072.

McKenna, A.M., R.K. Nelson, C.M. Reddy, J.J. Savory, N.K. Kaiser, J.E. Fitzsimmons, A.G. Marshall, and R.P. Rodgers. 2013. Expansion of the analytical window for oil spill characterization by ultrahigh resolution mass spectrometry: Beyond gas chromatography. *Environmental Science & Technology* 47(13):7,530–7,539, http://dx.doi.org/10.1021/es305284t.

Mendelssohn, I.A., G.L. Andersen, D.M. Baltz, R.H. Caffey, K.R. Carman, J.W. Fleeger, S.B. Joye, Q. Lin, E. Maltby, E.B. Overton, and L.P. Rozas. 2012. Oil impacts on coastal wetlands: Implications for the Mississippi River Delta ecosystem after the Deepwater Horizon oil spill. *BioScience* 62(6):562–574, http://dx.doi.org/10.1525/bio.2012.62.6.7.

Minchew, B., C.E. Jones, and B. Holt. 2012. Polarimetric analysis of backscatter from the Deepwater Horizon oil spill using L-band synthetic aperture radar. *IEEE Transactions on Geoscience and Remote Sensing* 50(10):3,812–3,830, http://dx.doi.org/10.1109/TGRS.2012.2185804.

Montagna, P.A., J.G. Baguley, C. Cooksey, I. Hartwell, L.J. Hyde, J.L. Hyland, R.D. Kalke, L.M. Kracker, M. Reuscher, and A.C. Rhodes. 2013. Deep-sea benthic footprint of the Deepwater Horizon blowout. *PloS ONE* 8:e70540, http://dx.doi.org/10.1371/journal.pone.0070540.

Murray, J.A., L.C. Sander, S.A. Wise, and C.M. Reddy. 2016. *Gulf of Mexico Research Initiative 2014/2015 Hydrocarbon Intercalibration Experiment: Description and Results for SRM 2779 Gulf of Mexico Crude Oil and Candidate SRM 2777 Weathered Gulf of Mexico Crude Oil.* National Institute of Standards and Technology (NIST) Interagency/Internal Report 8123, 331 pp., http://dx.doi.org/10.6028/NIST.IR.8123.

Nelson, R.K., C. Aeppli, J.S. Arey, H. Chen, A.H. de Oliveira, C. Eiserbeck, G.S. Frysinger, R.B. Gaines, K. Grice, J. Gros, and others. 2016. Applications of comprehensive two-dimensional gas chromatography (GC×GC) in studying the source, transport, and fate of petroleum hydrocarbons in the environment. Chapter 8 in *Standard Handbook of Oil Spill Environmental Forensics*. S.A. Stout and Z. Wang, eds, Elsevier.

Nixon, Z., S. Zengel, M. Baker, M. Steinhoff, G. Fricano, S. Rouhani, and J. Michel. 2016. Shoreline oiling from the Deepwater Horizon oil spill. *Marine Pollution Bulletin* 107:170–178, http://dx.doi.org/10.1016/j.marpolbul.2016.04.003.

NOAA Hazmat. 2012. Open water oil identification job aid for aerial observation. *Office of Response and Restoration Job Aid*. Version 2, http://response.restoration.noaa.gov/sites/default/files/OWJA_2012.pdf.

Overton, E.B., M.S. Miles, B.M. Meyer, H. Gao, and R.E. Turner. 2014. Oil source fingerprinting in heavily weathered residues and coastal marsh samples. Pp. 2,074–2,082 in *International Oil Spill Conference Proceedings,* vol. 2014, http://dx.doi.org/10.7901/2169-3358-2014.1.2074.

Passow, U., and K. Ziervogel. 2016. Marine snow sedimented oil released during the Deepwater Horizon spill. *Oceanography* 29(3):118–125, http://dx.doi.org/10.5670/oceanog.2016.76.

Pendergraft, M.A., Z. Dincer, J.L. Sericano, T.L. Wade, J. Kolasinski, and B.E. Rosenheim. 2013. Linking ramped pyrolysis isotope data to oil content through PAH analysis. *Environmental Research Letters* 8(4):044038, http://dx.doi.org/10.1088/1748-9326/8/4/044038.

Radović, J.R., C. Aeppli, R.K. Nelson, N. Jimenez, C.M. Reddy, J.M. Bayona, and J. Albaigés. 2014. Assessment of photochemical processes in marine oil spill fingerprinting. *Marine Pollution Bulletin* 79(1):268–277, http://dx.doi.org/10.1016/j.marpolbul.2013.11.029.

Ramseur, J.L. 2010. *Deepwater Horizon Oil Spill: The Fate of the Oil*. Congressional Research Service 7-5700, R41531, 20 pp.

Reddy, C.M., J.S. Arey, J.S. Seewald, S.P. Sylva, K.L. Lemkau, R.K. Nelson, C.A. Carmichael, C.P. McIntyre, J. Fenwick, G.T. Ventura, and B.A. Van Mooy. 2012. Composition and fate of gas and oil released to the water column during the Deepwater Horizon oil spill. *Proceedings of the National Academy of Sciences of the United States of America* 109(50):20,229–20,234, http://dx.doi.org/10.1073/pnas.1101242108.

Ruddy, B.M., M. Huettel, J.E. Kostka, V.V. Lobodin, B.J. Bythell, A.M. McKenna, C. Aeppli, C.M. Reddy, R.K. Nelson, A.G. Marshall, and R.P. Rodgers. 2014. Targeted petroleomics: Analytical investigation of Macondo well oil oxidation products from Pensacola Beach. *Energy & Fuels* 28(6):4,043–4,050, http://dx.doi.org/10.1021/ef500427n.

Ryerson, T.B., K.C. Aikin, W.M. Angevine, E.L. Atlas, D.R. Blake, C.A. Brock, F.C. Fehsenfeld, R.S. Gao, J.A. de Gouw, D.W. Fahey, and J.S. Holloway. 2011. Atmospheric emissions from the Deepwater Horizon spill constrain air-water partitioning, hydrocarbon fate, and leak rate. *Geophysical Research Letters* 38, L07803, http://dx.doi.org/10.1029/2011GL046726.

Ryerson, T.B., R. Camilli, J.D. Kessler, E.B. Kujawinski, C.M. Reddy, D.L. Valentine, E. Atlas, D.R. Blake, J. de Gouw, S. Meinardi, and D.D. Parrish. 2012. Chemical data quantify Deepwater Horizon hydrocarbon flow rate and environmental distribution. *Proceedings of the National Academy of Sciences of the United States of America* 109(50):20,246–20,253, http://dx.doi.org/10.1073/pnas.1110564109.

SMART. 2006. *Special Monitoring of Applied Response Technologies Protocol Report*. National Oceanic and Atmospheric Administration, US Coast Guard, U.S. Environmental Protection Agency, 43 pp., http://response.restoration.noaa.gov/sites/default/files/SMART_protocol.pdf.

Socolofsky, S.A., E.E. Adams, M.C. Boufadel, Z.M. Aman, Ø. Johansen, W.J. Konkel, D. Lindo, M.N. Madsen, E.W. North, C.B. Paris, and D. Rasmussen. 2015. Intercomparison of oil spill prediction models for accidental blowout scenarios with and without subsea chemical dispersant injection. *Marine Pollution Bulletin* 96:110–126, http://dx.doi.org/10.1016/j.marpolbul.2015.05.039.

Sun, S., C. Hu, L. Feng, G. Swayze, J. Holmes, G. Graettinger, I. MacDonald, O. Garcia, and I. Leifer. 2015. Oil slick morphology derived from AVIRIS measurements of the Deepwater Horizon oil spill: Implications for spatial resolution requirements of remote sensors. *Marine Pollution Bulletin* 103:276–285, http://dx.doi.org/10.1016/j.marpolbul.2015.12.003.

Tarr, M.A., P. Zito, E.B. Overton, G.M. Olson, P.L. Adhikari, and C.M. Reddy. 2016. Weathering of oil spilled in the marine environment. *Oceanography* 29(3):126–135, http://dx.doi.org/10.5670/oceanog.2016.77.

Thessen, A.E., S. McGinnis, and E.W. North. 2016. Lessons learned while building the Deepwater Horizon database: Toward improved data sharing in coastal science. *Computers & Geosciences* 87:84–90, http://dx.doi.org/10.1016/j.cageo.2015.12.001.

US Coast Guard. 2006. *Incident Management Handbook*. US Department of Homeland Security, COMDTPUB P3120.17A, 372 pp., http://www.uscg.mil/hq/nsfweb/docs/FinalIMH18AUG2006.pdf.

US Coast Guard. 2011. *On Scene Coordinator Report Deepwater Horizon Oil Spill*. Submitted to the National Response Team, 222 pp., http://www.uscg.mil/foia/docs/dwh/fosc_dwh_report.pdf.

Valentine, D.L., G.B. Fisher, S.C. Bagby, R.K. Nelson, C.M. Reddy, S.P. Sylva, and M.A. Woo. 2014. Fallout plume of submerged oil from Deepwater Horizon. *Proceedings of the National Academy of Sciences of the United States of America* 111(45):15,906–15,911, http://dx.doi.org/10.1073/pnas.1414873111.

Wade, T.L., J.L. Sericano, S.T. Sweet, A.H. Knap, and N.L. Guinasso Jr. 2016. Spatial and temporal distribution of water column total polycyclic aromatic hydrocarbons (PAH) and total petroleum hydrocarbons (TPH) from the Deepwater Horizon (Macondo) incident. *Marine Pollution Bulletin* 103:286–293, http://dx.doi.org/10.1016/j.marpolbul.2015.12.002.

Wade, T.L., S.T. Sweet, J.L. Sericano, N.L. Guinasso, A.R. Diercks, R.C. Highsmith, V.L. Asper, D. Joung, A.M. Shiller, S.E. Lohrenz, and S.B. Joye. 2011. Analyses of water samples from the Deepwater Horizon oil spill: Documentation of the subsurface plume. Pp. 77–82 in *Monitoring and Modeling the Deepwater Horizon Oil Spill: A Record-Breaking Enterprise*. Y. Liu, A. Macfadyen, Z.-G. Ji, and R.H. Weisberg, eds, Geophysical Monograph Series, American Geophysical Union, Washington, DC, http://dx.doi.org/10.1029/2011GM001103.

Weber, T.C., A. De Robertis, S.F. Greenaway, S. Smith, L. Mayer, and G. Rice. 2012. Estimating oil concentration and flow rate with calibrated vessel-mounted acoustic echo sounders. *Proceedings of the National Academy of Sciences of the United States of America* 109(50):20,240–20,245, http://dx.doi.org/10.1073/pnas.1108771108.

White, H.K., P.Y. Hsing, W. Cho, T.M. Shank, E.E. Cordes, A.M. Quattrini, R.K. Nelson, R. Camilli, A.W. Demopoulos, C.R. German, and others. 2012. Impact of the Deepwater Horizon oil spill on a deep-water coral community in the Gulf of Mexico. *Proceedings of the National Academy of Sciences of the United States of America* 109(50):20,303–20,308, http://dx.doi.org/10.1073/pnas.1118029109.

White, H.K., C.M. Reddy, and T.I. Eglinton. 2008. Radiocarbon-based assessment of fossil fuel-derived contaminant associations in sediments. *Environmental Science & Technology* 42(15):5,428–5,434, http://dx.doi.org/10.1021/es800478x.

Wilson, R.M., J. Cherrier, J. Sarkodee-Adoo, S. Bosman, A. Mickle, and J.P. Chanton. 2015. Tracing the intrusion of fossil carbon into coastal Louisiana macrofauna using natural ^{14}C and ^{13}C abundances. *Deep Sea Research Part II* 129:89–95, http://dx.doi.org/10.1016/j.dsr2.2015.05.014.

Zhou, Z., L. Guo, A.M. Shiller, S.E. Lohrenz, V.L. Asper, and C.L. Osburn. 2013. Characterization of oil components from the Deepwater Horizon oil spill in the Gulf of Mexico using fluorescence EEM and PARAFAC techniques. *Marine Chemistry* 148:10–21, http://dx.doi.org/10.1016/j.marchem.2012.10.003.

AUTHORS
Helen K. White (hwhite@haverford.edu) is Associate Professor of Chemistry, Haverford College, Haverford, PA, USA. **Robyn N. Conmy** is Ecologist, US Environmental Protection Agency, Cincinnati, OH, USA. **Ian R. MacDonald** is Professor, Florida State University, Tallahassee, FL, USA. **Christopher M. Reddy** is Senior Scientist, Woods Hole Oceanographic Institution, Woods Hole, MA, USA.